Springer Series in Solid-State Sciences 177

Alberto Bramati
Michele Modugno *Editors*

Physics of Quantum Fluids

New Trends and Hot Topics in Atomic and Polariton Condensates

Springer

Springer Series in
SOLID-STATE SCIENCES 177

Springer Series in

SOLID-STATE SCIENCES

The Springer Series in Solid-State Sciences consists of fundamental scientific books prepared by leading researchers in the field. They strive to communicate, in a systematic and comprehensive way, the basic principles as well as new developments in theoretical and experimental solid-state physics.

Alberto Bramati • Michele Modugno
Editors

Physics of Quantum Fluids

New Trends and Hot Topics in Atomic and Polariton Condensates

Springer

ISSN 0171-1873 Springer Series in Solid-State Sciences
ISBN 978-3-642-37568-2 ISBN 978-3-642-37569-9 (eBook)
DOI 10.1007/978-3-642-37569-9
Springer Heidelberg New York Dordrecht London

Library of Congress Control Number: 2013944213

Printed on acid-free paper

Springer is part of Springer Science+Business Media (www.springer.com)

Preface

The concept of *quantum fluid*—a fluid whose properties are governed by the laws of quantum mechanics—dates back to 1926, when Madelung introduced the hydrodynamic formulation of the Schrödinger equation. This, along with the prediction of Bose-Einstein condensation (BEC) for a non-interacting gas made by Einstein in 1924, and the discovery of superfluidity in liquid helium, achieved independently by Kapitza and Allen in 1937, can be considered the early milestones of this fashinating field.

Remarkably, though the role of Bose-Einstein condensation in the superfluid behaviour of helium was soon recognized by London in 1938, it took seventy year before its first direct observation. In fact, it was only in 1995 that the groups of Cornell, Weiman, and Ketterle achieved to cool a sample of atomic gases down to temperatures of the orders of few hundreds of nanokelvins, below the critical temperature for BEC. These landmark experiments have produced a tremendous impact in the experimental and theoretical research in the field of quantum fluids. In fact, thanks to the fact that interacting Bose-Einstein condensates (BECs) are genuine superfluids and that they can be controlled and manipulated with high precision, they have made possible to investigate thorougly many of the manifestation of superfluidity, as quantized vortices, absence of viscosity, reduction of the moment of inertia, occurrence of persistent currents, to mention a few.

Very recently, in 2006, following a pioneering proposal by Imamoglou (1996), BEC was observed in a solid state system: polaritons in semiconductor microcavities, which are composite bosons arising from the strong coupling between excitons and photons. Due to their very light mass, several orders of magnitude smaller than the free electron mass, polaritons can exhibit Bose-Einstein condensation at higher temperature and lower densities compared to atomic condensates. On the other hand, polaritons constitute a new type of quantum fluid with specific characteristics coming from its intrinsic dissipative and non-equilibrium nature.

The main objective of this book is to take a snapshot of the state of the art of this fast moving field with a special emphasis on the hot-topics and new trends. Bringing together the contributions of some of the most active specialists of the two areas (atomic and polaritonic quantum fluids), we expect that this work could facilitate

the exchanges and the collaborations between these two communities working on subjects with very strong analogies. The book is organized in two distinct parts, preceded by a general introduction; the first part is focussed on polariton quantum fluids and the second one is dedicated to the atomic BEC.

In the introductory chapter, M. Wouters gives an overview of the physics of the Bose-Einstein condensates of ultracold atoms and polaritons underlining their analogies and differences. This chapter reviews the main achievements and discusses the current trends of both fields.

Chapter 2 by N.G. Berloff and J. Keeling deals with the central problem of the universal description for the non-equilibrium polariton condensates. A special attention is paid to the theoretical framework describing the pattern formation in such systems. Different equations characterizing various regimes of the dynamics of exciton-polariton condensates are reviewed: the Gross-Pitaevskii equation which models the weakly interacting condensates at equilibrium, the complex Ginsburg-Landau equation which describes the behaviour of the systems in presence of symmetry-breaking instabilities and finally the complex Swift-Hohenberg equation. The authors also show how these equations can be derived from a generic laser model based on Maxwell-Bloch equations.

In Chap. 3, A. Kavokin develops a general theory for the bosonic spin transport that can be applied to different condensed matter systems like indirect excitons in coupled quantum wells and exciton-polaritons in semiconductor microcavities. The relevance of this approach to the emerging field of Spin-optronics in which the spin currents are carried by neutral bosonic particles is discussed and fascinating perspectives like spin-superfluidity are addressed.

Chapters 4 and 5 are focussed on the theoretical description of the properties of the spinor polariton condensates with a special emphasis on the occurrence of topological excitations in these fluids. In Chap. 4 by Y.G. Rubo, a review of the spin-dependent properties of the multi-component polariton condensates is presented. Special attention is devoted to describe the effect of applied magnetic fields on the polarization properties of the condensate; fractional vortices are discussed and the spin texture of the half-vortices in presence of the longitudinal-transverse splitting is discussed in detail. In Chap. 5, H. Flayac, D.D. Solnyshkov and G. Malpuech first discuss in detail the specific behaviour of a flowing spinor polariton allowing for the generation of a new kind of topological excitations: the oblique half solitons. In the second part of the chapter the authors show that these systems are extremely promising to study exotic entities analogue to the astrophysical black holes and wormholes.

Chapters 6 and 7 deal with experimental studies of hydrodynamics of polariton quantum fluids. In Chap. 6, B. Deveaud, G. Nardin, G. Grosso and Y. Léger describe the behaviour of a flowing polariton quantum fluid perturbed by the interaction with a potential barrier: this experimental configuration is well suited to investigate the onset of quantum turbulence in a quantum fluid. The variations of the phase and density of the fluid are measured with a picosecond resolution allowing for the observation of the nucleation of quantized vortices and the decay of dark solitons into vortex streets. In Chap. 7, D. Ballarini, A. Amo, M. de Giorgi

and D. Sanvitto review the first observations of superfluidity in a polariton fluid: the most relevant manifestations of the superfluid behaviour of these systems are discussed, namely the friction-less motion with the consequent scattering suppression in the Landau picture and the establishment of persistent currents in the case of rotating condensates. Moreover, the authors discuss the interesting regime of the superfluidity breakdown when the polariton fluid hits a spatially extended obstacle that can be natural or created in a controlled way by mean of well suited optical beams. Vortex nucleation, vortex trapping as well as the formation of oblique dark solitons are analysed in detail. In the last part of the chapter the authors show that the strong non-linearities of the polariton systems, together with their specific propagation properties can be exploited to develop a new class of optoelectronic devices for the classical and quantum information processing.

Chapters 8 and 9 are focussed on the properties of polariton condensates confined in low dimensional structures. In Chap. 8, N.Y. Kim, Y. Yamamoto, S. Utsunomiya, K. Kusudo, S. Höfling and A. Forchel discuss the properties of exciton-polaritons condensates in artificial traps and lattices geometries in various dimensions (0D, 1D and 2D). They show how coherent π-state with p-wave order in one dimensional condensate array and d-orbital state in two dimensional square lattices can be obtained. The authors point out the interest of preparing high-orbital condensates to probe quantum phase transitions and to implement quantum emulation applications. In Chap. 9, J. Bloch reviews the recent experiments performed with polariton condensates in low-dimensional microstructures. The propagation properties of polariton condensates confined in 1D microwires, together with the possibility to manipulate and control these condensates by optical means, are discussed in detail. In the second part of the chapter, the author shows how the study of polariton condensates in fully confined geometries, obtained in single or coupled micropillars, allows gaining a deep physical insight in the nature of interactions inside the condensate as well as with the environment. In the final part of the chapter, the interesting perspectives opened by the confined polariton condensates for the implementation of devices with new functionalities are briefly reviewed.

While the previous chapters are mainly focussed on the polariton quantum fluids in GaAs-based microstructures where a cryogenic temperature (4K) is needed, Chaps. 10 and 11 explore the possibilities opened by other materials to achieve polariton condensates at room temperature. Chapter 10 by J. Levrat, G. Rossbach, R. Butté and N. Grandjean presents the recent observation of the polariton condensation at room temperature (340 K) in GaN-based planar microcavities and analyses in detail the threshold of the polariton condensation phase transition as a function of the temperature and detuning. The role of the spin-anisotropy in the polariton-polariton interactions and its impact on the polarization properties of the condensate are comprehensively discussed. In Chap. 11, F. Médard, A. Trichet, Z. Chen, L.S. Dang and M. Richard present the recent progresses towards polariton condensation at room temperature in large band-gap nanostructures, namely ZnO nanowires. The unusually large Rabi splitting observed in these systems allows achieving stable polariton at room temperature, strongly decoupled from thermal fluctuations coming from lattice vibrations. Despite this behaviour, the authors show several experimental indications of polariton quantum degeneracy at room temperature.

Chapter 12, by F. Piazza, L.A. Collins, and A. Smerzi, opens the second part of the book, dedicated to the properties of quantum fluids made by ultracold atoms. In this chapter the authors discuss the dynamics of superfluid dilute Bose-Einstein condensates in the regime where the flow velocity reaches a critical value above which stationary currents are impossible. They present results for two- and three-dimensional BECs in two different geometries: a torus and a waveguide configuration, and also discuss the behavior of the critical current, establishing a general criterion for the breakdown of stationary superfluid flows.

Chapters 13 and 14 are devoted to turbolence effects in atomic BECs, that are particularly appealing as quantized vortices can be directly visualized and the interaction parameters can be controlled by Feshbach resonances. In Chap. 13, M. Tsubota and K. Kasamatsu review recent important topics in quantized vortices and quantum turbulence in atomic BECs, providing an overview of the dynamics of quantized vortices, hydrodynamic instability, and quantum turbulence. In Chap. 14, V.S. Bagnato et al. discuss their recent observations of quantum turbolence with a condensate of ^{87}Rb.

In Chap. 15, Y. Castin and A. Sinatra discuss the coherence of a three-dimensional spatially homogeneous Bose-condensed gas, initially prepared at finite temperature and then evolving as an isolated interacting system. They review different theoretical approaches, as the number-conserving Bogoliubov approach that allows to describe the system as a weakly interacting gas of quasi-particles, and the kinetic equations describing the Beliaev-Landau processes for the quasi-particles. They show that the variance of the condensate phase-change at long times is the sum of a ballistic term and a diffusive term, with temperature and interaction dependent coefficients, and discuss their scaling behaviors in the thermodynamic limit.

Chapter 16, by R.P. Smith and Z. Hadzibabic, review the role of interactions in Bose-Einstein condensation, covering both theory and experiments. They focus on harmonically trapped ultracold atomic gases, but also discuss how these results relate to the uniform-system case, which may be relevant for other experimental systems, and for theory in general. Despite the fact that the phase transition to a Bose-Einstein condensate can occur in an ideal gas, interactions are necessary for any system to reach thermal equilibrium and so are required for condensation to occur in finite time. The authors discuss this point clarifying the effects of interactions both on the mechanism of condensation and on the critical temperature, and then review the conditions for measuring the equilibrium thermodynamics. They also discuss the non-equilibrium phenomena that occur when these conditions are controllably violated by tuning the interparticle-interaction strength.

In Chap. 17, T. Mukaiyama and M. Ueda provide an overview of theories and experiments on the thermodynamics of Fermi gases at unitarity, where the scattering length diverges, that is characterized by a universal behavior.

Finally, in Chap. 18, G. Barontini and H. Ott introduce the scanning electron microscopy (SEM), that represents one of the most promising techniques for probing and manipulating ultracold atomic systems with extremely high resolution and precision. Thanks to its extremely high resolution, below 100 nm, and to the single-atom sensitivity, the SEM method permits the observation of in-situ

profiles of trapped Bose-Einstein condensates and of ultracold clouds in one- and two-dimensional optical lattices. Moreover, the single lattice sites can be selectively addressed and manipulated in order to create arbitrary patterns of occupied sites.

We hope this book will be a useful introduction to a wide audience of researchers who wish to approach the physics of quantum fluids and be updated on the last fascinating achievements in this cutting-edge research field. Last but not least, we would like to thank all the contributors for their effort in making this project possible.

Paris, France — Alberto Bramati
Bilbao, Spain — Michele Modugno

Contents

Contributors

A. Amo Laboratoire de Photonique et de Nanostructures, CNRS, Marcoussis, France

G. Bagnato Instituto de Física de São Carlos, Universidade de São Paulo, São Carlos, SP, Brazil

V.S. Bagnato Instituto de Física de São Carlos, Universidade de São Paulo, São Carlos, SP, Brazil

D. Ballarini Istituto Italiano di Technologia, IIT-Lecce, Lecce, Italy; Istituto Nanoscienze – CNR, NNL, Lecce, Italy

Giovanni Barontini Research Center OPTIMAS and Fachbereich Physik, Technische Universität Kaiserslautern, Kaiserslautern, Germany

N.G. Berloff Department of Applied Mathematics and Theoretical Physics, University of Cambridge, Cambridge, UK

Jacqueline Bloch Laboratoire de Photonique et de Nanostructures, LPN/CNRS, Marcoussis, France

Raphaël Butté Institute of Condensed Matter Physics, Ecole Polytechnique Fédérale de Lausanne, Lausanne, Switzerland

M. Caracanhas Instituto de Física de São Carlos, Universidade de São Paulo, São Carlos, SP, Brazil

Yvan Castin Laboratoire Kastler Brossel, Ecole normale supérieure, CNRS and UPMC, Paris, France

Z. Chen Surface Physics Laboratory, Department of Physics, Fudan University, Shanghai, China

L.A. Collins Theoretical Division, Los Alamos National Laboratory, Los Alamos, NM, USA

L.S. Dang Institut Néel, CNRS-CEA, Grenoble, France

M. de Giorgi Istituto Italiano di Technologia, IIT-Lecce, Lecce, Italy; Istituto Nanoscienze – CNR, NNL, Lecce, Italy

Benoit Deveaud Ecole Polytechnique Fédérale de Lausanne, Lausanne, Switzerland

Hugo Flayac Clermont Université and Université Blaise Pascal, LASMEA, Nanostructure and Nanophotonics Group, CNRS, Aubière Cedex, France

Alfred Forchel Technische Physik and Wilhelm-Conrad-Röntgen-Research Center for Complex Material Systems, Universität Würzburg, Würzburg, Germany

Nicolas Grandjean Institute of Condensed Matter Physics, Ecole Polytechnique Fédérale de Lausanne, Lausanne, Switzerland

Gabriele Grosso Ecole Polytechnique Fédérale de Lausanne, Lausanne, Switzerland

Zoran Hadzibabic Cavendish Laboratory, University of Cambridge, Cambridge, UK

E.A.L. Henn Instituto de Física de São Carlos, Universidade de São Paulo, São Carlos, SP, Brazil

Sven Höfling Technische Physik and Wilhelm-Conrad-Röntgen-Research Center for Complex Material Systems, Universität Würzburg, Würzburg, Germany

Kenichi Kasamatsu Department of Physics, Kinki University, Higashi-Osaka, Japan

Alexey Kavokin Spin Optics Laboratory, St-Petersburg State University, St-Petersburg, Russia; Physics and Astronomy School, University of Southampton, Southampton, UK

J. Keeling School of Physics and Astronomy, University of St Andrews, SUPA, St Andrews, UK

Na Young Kim E. L. Ginzton Laboratory, Stanford University, Stanford, CA, USA

Kenichiro Kusudo National Institute of Informatics, Chiyoda-ku, Tokyo, Japan

Jacques Levrat Institute of Condensed Matter Physics, Ecole Polytechnique Fédérale de Lausanne, Lausanne, Switzerland

Yoan Léger Ecole Polytechnique Fédérale de Lausanne, Lausanne, Switzerland

K.M.F. Magalhães Instituto de Física de São Carlos, Universidade de São Paulo, São Carlos, SP, Brazil

Guillaume Malpuech Clermont Université and Université Blaise Pascal, LASMEA, Nanostructure and Nanophotonics Group, CNRS, Aubière Cedex, France

F. Médard Institut Néel, CNRS-CEA, Grenoble, France

Takashi Mukaiyama Institute for Laser Science, University of Electro-Communications, Chofu, Tokyo, Japan

S.R. Muniz Instituto de Física de São Carlos, Universidade de São Paulo, São Carlos, SP, Brazil

Gael Nardin Ecole Polytechnique Fédérale de Lausanne, Lausanne, Switzerland

Herwig Ott Research Center OPTIMAS and Fachbereich Physik, Technische Universität Kaiserslautern, Kaiserslautern, Germany

F. Piazza INO-CNR, BEC Center and Dipartimento di Fisica, Università di Trento, Povo, Trento, Italy

M. Richard Institut Néel, CNRS-CEA, Grenoble, France

G. Roati LENS and Dipartimento di Fisica, Università di Firenze, and INFM-CNR, Sesto Fiorentino, Italy

Georg Rossbach Institute of Condensed Matter Physics, Ecole Polytechnique Fédérale de Lausanne, Lausanne, Switzerland

Y.G. Rubo Instituto de Energías Renovables, Universidad Nacional Autónoma de México, Temixco, Morelos, Mexico

D. Sanvitto Istituto Italiano di Technologia, IIT-Lecce, Lecce, Italy; Istituto Nanoscienze – CNR, NNL, Lecce, Italy

J.A. Seman LENS and Dipartimento di Fisica, Università di Firenze, and INFM-CNR, Sesto Fiorentino, Italy

R.F. Shiozaki Instituto de Física de São Carlos, Universidade de São Paulo, São Carlos, SP, Brazil

Alice Sinatra Laboratoire Kastler Brossel, Ecole normale supérieure, CNRS and UPMC, Paris, France

A. Smerzi INO-CNR, BEC Center and Dipartimento di Fisica, Università di Trento, Povo, Trento, Italy

Robert P. Smith Cavendish Laboratory, University of Cambridge, Cambridge, UK

Dmitry D. Solnyshkov Clermont Université and Université Blaise Pascal, LASMEA, Nanostructure and Nanophotonics Group, CNRS, Aubière Cedex, France

P. Tavares Instituto de Física de São Carlos, Universidade de São Paulo, São Carlos, SP, Brazil

G. Telles Instituto de Física de São Carlos, Universidade de São Paulo, São Carlos, SP, Brazil

A. Trichet Institut Néel, CNRS-CEA, Grenoble, France

Makoto Tsubota Department of Physics, Osaka City University, Osaka, Japan

Masahito Ueda Department of Physics, University of Tokyo, Bunkyo-ku, Tokyo, Japan

Shoko Utsunomiya National Institute of Informatics, Chiyoda-ku, Tokyo, Japan

Michiel Wouters TQC, Universiteit Antwerpen, Antwerpen, Belgium

Yoshihisa Yamamoto E. L. Ginzton Laboratory, Stanford University, Stanford, CA, USA; National Institute of Informatics, Chiyoda-ku, Tokyo, Japan

Chapter 1
Quantum Fluids of Exciton-Polaritons and Ultracold Atoms

Michiel Wouters

Abstract We give an overview of the physics of quantum degenerate Bose gases of ultracold atoms and of exciton polaritons in microcavities. The physical systems are described and the main experimentally accessible observables are outlined. We give a schematic overview of recent trends in both fields.

1.1 Introduction

The physics of the quantum Bose gases took off from the theoretical side, when Einstein predicted that the bosonic statistics induces a phase transition in a noninteracting gas at low temperatures, when the interparticle distance is comparable to the de Broglie wave length [39]. Below the transition temperature, the gas enters the Bose-Einstein (BE) condensed phase, where a macroscopic number of particles occupies the lowest momentum state, leading to the coherence of the phase over macroscopic distances. The first physical example of this type of transition was superfluid Helium. Due to the strong interactions between the Helium atoms however, its theoretical description is complicate and the connection to the ideal Bose gas is not so direct. Still the macroscopic phase coherence and superfluidity are not qualitatively altered by the strength of interactions, so that the ideal Bose gas remains conceptually a good starting point to understand the remarkable behavior of superfluid Helium. It was in this context that Bogoliubov analyzed the effect of weak interactions and Pitaevskii constructed the classical theory for inhomogeneous Bose-Einstein condensates.

A physical realization of the weakly interacting Bose gas was lacking for many years. The condition of weak interactions $nR_e^3 \ll 1$ is only satisfied when the interparticle distance ($n^{-1/3}$) is much larger than the range of the interactions (R_e). No gases satisfy this condition at thermodynamic equilibrium. Several ideas were pursued to create metastable quantum gases that are in the weakly interacting limit. Both excitons in semiconductors and very dilute atomic gases were conceived to

M. Wouters (✉)
TQC, Universiteit Antwerpen, Universiteitsplein 1, 2610 Antwerpen, Belgium
e-mail: michiel.wouters@ua.ac.be

A. Bramati, M. Modugno (eds.), *Physics of Quantum Fluids*,
Springer Series in Solid-State Sciences 177, DOI 10.1007/978-3-642-37569-9_1,

be good candidates to achieve this goal. The first successful realization was obtained with dilute atoms in 1995 [13]. The condensation of excitons on the other hand proved to be much harder due to the complicated solid state environment. By coupling the exciton to a cavity photon, polariton quasi-particles are created. Because of their much lighter mass as compared to the exciton, they are much easier to condense in the ground state. Unambiguous proof hereof was obtained in 2006 [28].

The ultracold dilute atomic gases have turned out a very flexible system, and can be used as emulators for a wide variety of quantum systems and the field has witnessed a vigorous expansion. It is beyond the scope of the present introduction to cover this field. We will rather restrict ourselves to the physics of bosonic atoms in the regime of weak interactions. On the polariton side, the relative simplicity of the experiments has allowed for many milestone experiments to be performed in a relatively short time. The field being still much smaller than the cold atom one, we will cover relatively more of the polariton physics.

1.2 The Systems

In the following sections, we will start with short separate introductions to the microcavity and cold atom systems to describe their specific features.

1.2.1 The Microcavity Polariton System

1.2.1.1 Microcavity Polariton Properties

A microcavity is a solid state Fabri-Perrot cavity with a distance between the mirrors of the order of one micron. The mirrors are flat so that the photon modes have a conserved momentum in the directions parallel to the mirror plane, making them a two-dimensional (2D) system. At small momenta, their dispersion is in good approximation quadratic $\omega_C(k) = \omega_C^0 + k^2/2m_C$, where the effective mass is four orders of magnitude smaller than the free electron mass $m_C = 10^{-4}m_e$. The resonance frequency ω_C^0 is in the electron volt range, the typical energy scale of electronic transitions. The mirrors are usually Distributed Bragg reflectors (DBRs) with a quality factor of the order of 10.000, yielding photon line widths in the 0.1 meV range, corresponding to a few ps life time [15].

When a material is placed between the mirrors, that has an electronic transition in resonance with the optical mode, the electronic excitations couple to the light. Of particular interest is the coupling to an excitonic transition (bound electron hole pair) in the material, illustrated in Fig. 1.1(a). When a photon creates an exciton, the center of mass momentum of the exciton is equal to the photon momentum. The relative wave function of the exciton being fixed, the coupling between a photon and exciton at momentum $\mathbf{k}$ can be seen as the coupling in a two-level system. In

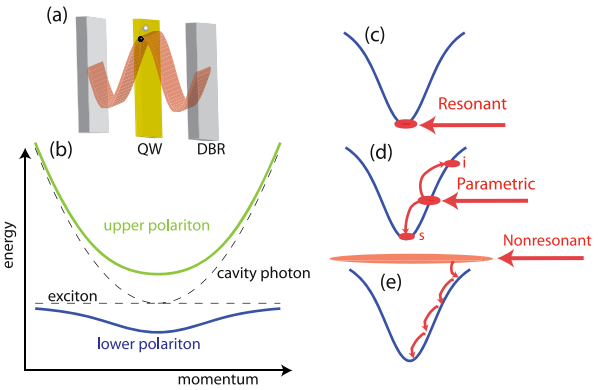

Fig. 1.1 (**a**) Overview of the microcavity polariton system. A cavity photon is strongly coupled to an exciton transition in an embedded quantum well. (**b**) The dispersion of the upper (*green*) and lower (*blue*) polaritons, compared to the bare exciton and photon dispersions (*dashed lines*). (**c**), (**d**), (**e**) comparison of the different excitation schemes: resonant (**c**), parametric (**d**) and nonresonant (**e**)

second quantization, this coupling can be described by a term in the Hamiltonian of the form

$$H_R = \frac{\Omega_R}{2} \sum_{\mathbf{k}} \psi_C^\dagger(\mathbf{k}) \psi_X(\mathbf{k}) + h.c. \tag{1.1}$$

where the coupling parameter Ω_R is the Rabi frequency and ψ_C annihilates a cavity photon. The operator ψ_C describes the annihilation of an exciton (electron-hole pair). To enhance the binding energy, the exciton is usually confined in a quantum well. The eigenstates of the full linear Hamiltonian $H = H_0 + H_R$, with the free Hamiltonian

$$H_0 = \sum_{\mathbf{k}} \left[\omega_C(k)\, \psi_C^\dagger(\mathbf{k}) \psi_C(\mathbf{k}) + \epsilon_X\, \psi_X^\dagger(\mathbf{k}) \psi_X(\mathbf{k}) \right], \tag{1.2}$$

can be obtained by diagonalizing it at fixed $\mathbf{k}$. The dispersion of the quasi-particles, the so-called lower and upper polaritons, is shown in Fig. 1.1(b). The splitting between upper and lower polariton was first experimentally seen by Weisbuch et al. in 1992 [56]. Note that in (1.2), we have neglected the momentum dependence of the exciton energy, which is well justified since its mass is around four orders of magnitude heavier than the cavity photon.

The coupling between excitons and photons is determined by the Rabi frequency Ω_R, that is of the order of a few meV in GaAs up to 50 meV in GaN (discussed in Chap. 10), 130 meV in ZnO (see Chap. 11) and even higher in organic materials [1]. A larger Rabi frequency makes the polaritons more robust with respect to temperature. Experiments with GaAs microcavities are conducted at cryogenic temperatures around 10 K, where polaritons in GaN (see Chap. 10) and organic materials can be observed at room temperature. Many experiments are however conducted with GaAs microcavities, because the growth technology for this material is much

more advanced thanks to its use in commercial opto-electronic applications. Much progress has however been made in the fabrication of GaN microcavities and many of the pioneering experiments on polariton condensation have been conducted on a CdTe microcavity [28, 33, 42].

The microcavities are structurally identical to Vertical Cavity Surface Emitting Lasers (VCSELs). The only difference is that their excitonic resonance is carefully tuned to the cavity photon. The most important consequence hereof is that unlike photons, the polaritons interact significantly with each other. Indeed, the excitons consist of electrons and holes and their (exchange dominated) interaction is responsible for the polariton-polariton interactions [11]. It is theoretically modeled by adding the interaction term

$$H_I = \frac{g}{2}\int d\mathbf{x}\, \psi_X^\dagger(\mathbf{x})\psi_X^\dagger(\mathbf{x})\psi_X(\mathbf{x})\psi_X(\mathbf{x}) \tag{1.3}$$

to the Hamiltonian. Its approximation by a contact interaction is well justified, because the range of the exciton-exciton interaction potential is of the order of 10 nm, where the polariton physics takes place on the μm length scale.

On resonance, the polariton is half exciton and half photon, so that the effective polariton-polariton interaction is $g_{LP} = g/4$. The relevant dimensionless coupling constant that characterizes the strength of interactions in a 2D gas of particles with mass m is $\tilde{g} = mg/\hbar^2$ [7]. This means that even though the excitons are in a regime of strong interactions $\tilde{g} = m_X g/\hbar^2 \sim 1$, the polaritons are in a weakly interacting regime. For example in GaAs microcavities, the dimensionless interaction constant is of the order of $\tilde{g} = m_{LP} g/\hbar^2 \approx 0.01$.

A second major difference with the bare exciton gas concerns the role of disorder. A certain degree of disorder due to growth fluctuations is inevitable. Fluctuations in the quantum well width result in an inhomogeneous effective potential for the excitons, with a correlation length on the nm scale and gives a inhomogeneous linewidth in the order of one meV. It however turns out that when the Rabi frequency is larger than this inhomogeneous broadening, the polariton modes are quite insensitive to the excitonic disorder [45]. The major source of disorder acting on the polaritons comes from the fluctuation in the distance between the two DBR mirrors. A monolayer fluctuation gives an energy shift of the order of 0.5 meV, which is of the same order of magnitude as the other polariton energy scales.

Controllable manipulation of the potential acting on the polaritons is possible by a variety of techniques, that are discussed in Chap. 8. Among the most successful strategies of creating potentials acting on the polaritons are etching (see Chaps. 8 and 9), stress induced traps [4], surface acoustic waves [10] and controlled variation of the DBR thickness (see Chap. 6).

So far, we have simplified the discussion by neglecting the polarization degree of freedom of the polaritons [47]. The photon however has two polarization states. In GaAs for example, there are four exciton polarization states. The photon only couples to the $m_z = \pm 1$ excitons. The other two states with $m_z = \pm 2$ are not coupled to the light because of angular momentum conservation. They are dark and do not form polaritons.

The single particle polariton eigenstates have a well defined linear polarization due to the splitting of both the photon and exciton linear polarization states. For what concerns the polariton-polariton interactions however, the conservation of angular momentum in collisions results in the conservation of the circularly polarized states. The interactions turn out to be anisotropic: the interactions between cocircular polarized polaritons is larger than between countercircularly polarized ones: $g_{\uparrow\uparrow} \gg |g_{\uparrow\downarrow}|$. This is due to the fact that the dominant contribution comes from the Pauli exclusion principle (exchange interaction). For countercircularly polarized excitons, both electron and hole spins are however different, so that the exchange contribution vanishes. The interactions due to higher order terms have been found to be negative $g_{\uparrow\downarrow} < 0$ [31, 54].

Discussions on the spin physics of polaritons can be found in Chaps. 3 and 4.

1.2.1.2 Experiments with Polaritons

In its ground state, the microcavity is empty. Polaritons can be injected by means of optical or electrical injection. The polariton life time is mainly limited by the finite photon life time. In state of the art microcavities, it is around 10 ps, which is of the order of the other time scales of their dynamics and thus presents a severe limitation. Therefore, polaritons are often continuously injected in order to compensate for these losses. Two different optical injection schemes should be distinguished. The first excitation scheme is *resonant* excitation (see Fig. 1.1(c)): A laser is tuned to the polariton frequency at a given wave vector. The second scheme is *nonresonant* excitation (see Fig. 1.1(e)). In this latter case, the laser is tuned to an energy above the polariton energy. High energy excitons or free electron-hole pairs are formed, that subsequently relax to the bottom of the lower polariton branch. Electrical excitation has a similar effect.

An important difference between the resonant and nonresonant excitation schemes concerns the $U(1)$ phase symmetry of the polariton field. In the case of resonant excitation, the coupling of the external laser amplitude F_L to the microcavity adds a term to the Hamiltonian

$$H_L = F_L e^{-i\omega_L t} \Psi^\dagger(\mathbf{k}_L) + h.c. \tag{1.4}$$

that explicitly breaks the $U(1)$ symmetry. The phase of the polariton field is determined by the phase of the laser and in particular its spatial and temporal coherence is determined by the coherence properties of the laser light. Under nonresonant excitation on the other hand, the $U(1)$ symmetry is not explicitly broken and polariton coherence can spontaneously form. Various models to describe this symmetry broken nonequilibrium state are discussed in Chap. 2.

An excitation scheme that is intermediate between resonant and nonresonant excitation is the so-called parametric excitation [25, 51]. The lower polariton branch is excited resonantly at an energy above the ground state carefully chosen so that polaritons can scatter into the ground state (signal) and an excited state (idler) through a single collision. The parametric scheme is illustrated in Fig. 1.1(d). Where under

parametric excitation, the phase of the pumped mode is fixed by the laser, the signal phase is chosen spontaneously, because only the sum of signal and idler phases is fixed $\phi_s + \phi_i = 2\phi_p$. Therefore, the spontaneous formation of coherence is observed when the density of polaritons in the signal mode is increased.

Finally, under pulsed resonant excitation, the polariton phase is only fixed as long as the laser pulse excites the microcavity and is free to evolve afterwards. The main limitation of this scheme is, as we mentioned earlier, the finite polariton life time that makes the density drop on the same time scale as the other time scales that are involved in the dynamics.

1.2.2 The Cold Atom System

Similar to polaritons, also the dilute clouds of ultracold alkali atoms are not in their ground state, which is the solid phase. The relaxation to a solid however needs three-body interactions, which are very slow at low densities and the gas phase is metastable with a life time that can be of the order of one minute. This is much longer than the time needed to reach thermal equilibrium and much longer than the typical time scales of the dynamics. It is therefore a good approximation to neglect the finite life time of the trapped atoms.

Since the realization of Bose-Einstein condensation, the field of ultracold atoms has witnessed an explosive growth. Nowadays, many experiments are performed on atoms of bosonic and fermionic [21] statistics, that can be combined with ions [61] and strongly coupled to light [8]. The scope of this chapter is limited to point out some aspects of the physics of ultracold bosonic gases. More extensive reviews of their properties can be found in several text books on the subject [38, 39]. Due to the three-body losses, the maximum density of the atoms is around $n = 10^{14}$ cm^{-3}. This means that the typical interatomic spacing is similar to the polariton spacing of around 1 micron. Quantum degeneracy is reached when the de Broglie wavelength reaches this value. Due to the much heavier atomic mass, the temperature requirement for the atoms is much more severe and of the order of 100 nK, eight orders of magnitude smaller than in the polariton case. Thanks to the excellent isolation of the atomic clouds from any environment, these ultralow temperatures can however be routinely achieved. While the BEC phase transition does not rely on the interactions between the atoms, the transition temperature is affected by atomic interactions (see Chap. 16).

Spin conservation laws in the collisions of atoms make that for several combinations of hyperfine states, the number of atoms in each state is conserved. Mixtures of a well defined number of atoms in each hyperfine state can thus be prepared, which allows to study atomic gases with tunable effective spin.

Interactions between ultracold atoms have a range that is of the order of 10 nm, much shorter than their spacing. The interaction can thus be well approximated by

a contact interaction, that reads in three dimensions (omitting technicalities concerning their regularization)

$$V(\mathbf{x}) = \frac{4\pi\hbar^2 a_{sc}}{m}\delta(\mathbf{r}), \tag{1.5}$$

where a_{sc} is the scattering length, that is typically of the order of the range of the interactions. Making use of so-called Feshbach resonances, the scattering length can be tuned at will. Both positive and negative signs for the scattering length can be reached. In absolute value, it can be tuned from zero to values larger than the interparticle spacing. In the latter regime, the atomic gas enters a very controlled strongly interacting regime.

An alternative route to the regime of strong interactions in bosons is by using optical lattices. These are periodic potentials generated by standing laser fields. They allow to realize a tunable bosonic Hubbard model, where the dramatic effects of interactions between bosonic particles were first evidenced in the superfluid to Mott insulator phase transition [22].

Interactions can be meaningfully compared between 2D polariton gases and 2D atomic clouds. The latter can be created by applying a standing laser field that confines the cloud in one dimension only. In experiments on the 2D Bose gas, the interaction strength is tunable and takes values in the range $\tilde{g} = 10^{-2}$–0.3 [12, 24, 26]. As discussed above, Microcavity polariton in GaAs microcavities are in the lower values of this range.

The coupling of ultracold gases to cavity photons has been achieved as well, making for a systems that is at first sight strongly analogous to the microcavity one. For example, in Ref. [8], a BEC was placed inside an optical cavity, that was tuned to an electronic transition of the atoms, a situation very similar to the quantum well embedded in a microcavity. An important difference between the two cases is the dimensionality of the photon. Where it has in the semiconductor case the same dimensionality as the exciton, in the atomic case, the photon is zero-dimensional where the condensate is 3D. A second ingredient that causes an important difference, where the motion of the Ga and As atoms is negligible for the crystalline solid state materials, the atoms move while they interact with the light, leading to optomechanical effects [8].

1.3 Observables

1.3.1 Microcavities

The measurement of the polariton state inside the microcavity is straightforward, thanks to the one-to-one correspondence between the microcavity polaritons and the light that is transmitted through the microcavity mirrors [46]. Using standard optical techniques, the polariton density can be measured in real space $n(\mathbf{x})$ or in

momentum space $n(\mathbf{k})$. Using a spectrometer, the energy spectrum is readily obtained, resulting in images of $n(\mathbf{x}, \omega)$ or $n(\mathbf{k}, \omega)$. When a streak camera is used, the time evolution of the density can be monitored with a ps resolution.

By interfering the light that is emitted at different positions, the spatial coherence $g^{(1)}(\mathbf{x}_1, \mathbf{x}_2) = \langle \psi^+(\mathbf{x}_1)\psi(\mathbf{x}_2)\rangle / \sqrt{n(\mathbf{x}_1)n(\mathbf{x}_2)}$ can be measured [28]. From the interferrograms, also the average phase difference between different regions in the condensate can be extracted. This has allowed to evidence the existence of quantized vortices in polariton condensates [32]. This interference technique to visualize vortices has been first used for atomic condensates by Inouye et al. [27].

It is important to point out that all the measurements of polariton gases are performed over times that are very long as compared to the polariton life time. For a steady state measurement, this means that actually a long time average is recorded. In practice, the cw experiments are performed with long pulses. A typical measurement takes a time that is long with respect to the pulse duration and thus averages over many realizations of the condensate. For the observation of vortices, this means that only an average phase profile is measured, that completely misses moving vortices. For pulsed experiments where the time evolution is followed, the measurements record the average over multiple realizations of the dynamics. Again, the particular trajectory of a single realization cannot be followed.

1.3.2 Ultracold Atoms

The main observable of ultracold atoms is the density: the atomic (column) density can be imaged through its absorption of laser light. It has turned out that from the density, combined with an engineered evolution of the system before recording it, an enormous wealth of information can be derived. The clearcut observation of BEC in 1995 was a density measurement performed a certain time after the trap was switched off. The free expansion maps approximately the momentum to the distance and thus gives a good estimate of the momentum distribution. A further analysis shows that the mapping of distance to momentum is modified by the interactions during the early stages of the expansion. Note that in the polariton case, the momentum distribution is also obtained by a kind of free expansion of the emitted photons. There however, interactions are always negligible, because the propagation takes fully place outside of the microcavity, where photon-photon interactions are absent.

Also from the *in situ* measurements of the atomic clouds, important information can be extracted. By using high resolution optical [48] or scanning electron microscopy (SEM) techniques, the atomic density profiles can be measured with a resolution that is better than the interparticle distance and the lattice spacing of optical lattices. Thanks to the single atom sensitivity, also higher order correlations can be measured. This technique will be described in Chap. 18.

A crucial difference between the measurements of ultracold atoms and polaritons is that in the case of the ultracold atoms information is obtained from a single

shot measurement. A picture of a single realization of the ensemble of atoms is taken. This is relevant for phase measurements. Two atomic clouds can be made to interfere with each other and a particular realization of an experiment will always show interference fringes, irrespective of whether the phases of the two clouds are related or not. This makes it straightforward to observe spontaneous vortices [24]. The presence of a vortex is signaled by a fork like dislocation in the interference pattern between the condensate and a reference condensate. By repeating such an experiment many times, the probability distribution for the number of vortices can be measured.

Spectral information on the Bose gases can be extracted by applying time-dependent laser fields. An example is Bragg spectroscopy [50]. In this type of experiments, two lasers with frequency difference $\Delta\omega$ and wave vector difference Δk are applied to the gas. A large response of the atoms is observed when $(\Delta k, \Delta\omega)$ coincides with a resonance in the structure factor. Another example is modulation spectroscopy, where the standing laser field that creates an optical lattice is modulated [52]. The excitation frequency and spectrum turns out to be a precise probe for the properties of the quantum fluid.

For the measurement of temporal coherence, Ramsey type experiments can be used. A proposal for the measurement of the temporal coherence of atomic condensates is discussed in Chap. 15.

1.4 Physical Properties

1.4.1 Condensate Shape

In contrast to conventional condensed matter systems such as the electron gas or superfluid Helium, both the ultracold atoms and polariton gases are strongly inhomogeneous. The overall trapping potential acting on cold atoms is usually well approximated by a quadratic potential. In the polariton case, not only trapping potentials can be present, but also the excitation that injects particles is inhomogeneous. The physical consequences of the inhomogeneity are very different for systems at thermodynamic equilibrium and for nonequilibrium gases.

In the case of cold atoms in equilibrium, the effect of a shallow quadratic trapping potential can in good approximation be described in the local density approximation. This means that the gas can be treated locally as homogeneous at a given chemical potential $\mu(\mathbf{r})$. This chemical potential varies in space as $\mu(\mathbf{r}) = \mu_0 - V_{ext}(\mathbf{r})$, where V_{ext} is the trapping potential. What at first sight could seem to be a complication, actually turns out to be a convenience: one has access to a range of chemical potentials in a single experiment. Measuring the local density, it is possible to extract the equation of state $\mu(n)$, from which thermodynamic quantities such as the pressure and phase space density can be extracted. A discussion on this method in the context of the unitary Fermi gas is given in Chap. 17.